Analecta Technica Szegedinensia
Vol. 18, No. 3 ISSN 2064-7964 2024

ANALYSIS OF THE SPANWISE EFFECT BEHIND A CYLINDRICAL BODY

[1]Bence Molnár, [2]Péter Bencs

[1,2]Department of Fluid and Heat Engineering, Faculty of Mechanical Engineering and Informatics, University of Miskolc, Miskolc-Egyetemváros, H-3515 Miskolc, Hungary,
Correspondence e-mail: peter.bencs@uni-miskolc.hu

Received: 14th June	*Accepted: 11th September*

ABSTRACT

The study of the flow around the cylinder is still a focus of research in various aspects. In this case, the flow around an electrically heated cylinder with a diameter Ø*d*=10 mm is investigated at low velocities (mainly in the laminar range). In the literature, the wall temperature Tw is used in many places to characterize such flows. This is usually considered constant, because experimental tests are mainly performed with electrically heated rods of small diameter (max ~2 mm). Since in our case the rod diameter is a multiple of this, the question arises whether the two-dimensional nature of the flow behind the cylinder is preserved. The spanwise effect behind a transversely placed heated cylinder was investigated. The results obtained provide a good basis for designing further measurement options.

Keywords: cylinder, spanwise, numerical simulation, PIV

1. INTRODUCTION

The results so far of the tests of the flow around a heated rod in a wind tunnel in the workshop hall of the Department of Fluid and Heat Engineering are presented. In our study, due to the nature of the particle image-based velocity determination device, the base flow in the wind tunnel was set to 0.3 m/s. The Reynolds number for the cylindrical heated rod can be calculated to determine the range of the flow. From the diameter of the rod to be heated (*d*=10 mm), the base flow velocity and the viscosity at ambient air temperature, the Reynolds number for the rod is Re_{rod}≈200.

It can be seen from the Reynolds number that the fluid flow is still laminar, but the vortices are now periodically separated from the two sides of the rod, thus forming a series of Kármán vortices. Since the flow is still laminar, the flow profile should be essentially the same in all planes along the longitudinal axis of the rod. If we consider the phenomenon as two-dimensional, we are looking at the flow around a circular section. If we extend this to three dimensions, then the model is effectively made up of many such slices, where the numerical simulation program calculates the flow pattern along the longitudinal axis of the cylinder and at each intersection, where the flow profile may be different for different intersections. This is the so-called spanwise phenomenon, where the question is therefore how much and how the nature of the flow changes, is there periodicity in each cross-section along the longitudinal axis of the bar. In this thesis, I investigate this phenomenon using a three-dimensional model, and the purpose of our measurements is to represent and study it.

The phenomenon has been observed by several researchers. Bernd et al. (1993) investigated vortices detaching from the cylinder in the Re=150 and 200 Reynolds number range, where they found three-dimensional (3D) instabilities in the two-dimensional flow at Re≈170 Reynolds number. Henderson and Barkley (1996) used the Floquet analysis of flow around a circular cylinder and identified two 3D instabilities: 'Mode A' A at Re ≈189 and 'Mode B' at Re ≈259 Reynolds numbers. Based on their results, it can be stated that for flow around a stationary cylinder with Re >190, a 3D method is required to accurately describe the flow. This fact was later confirmed by Leweke and Williamson (1998), who also found two 3D instabilities [1]. Thus, 3D instabilities appear in two-dimensional flow from Re≈170 (Bernd et al.), and for Reynolds numbers higher than this, a 3D method is needed to describe the flow accurately. Since in our experimental setup the Reynolds number Re≈200 is defined for the heated rod, we assume that 3D instabilities already appear in the flow.

DOI: https://doi.org/10.14232/analecta.2024.3.49-58

Instability is a non-linear problem that follows from the non-linear Navier-Stokes equations describing fluid motion, as the solution to these equations sometimes yields a step change. The reason is that non-linear equations are characterised by the fact that small changes in the parameters lead to large changes in the results in some cases. The reason why it is important to determine the exact occurrence of instabilities is that once the boundary where these instabilities occur is crossed, the flow is no longer two-dimensional, and therefore a 2D computational code cannot be used to describe the flow because it will not be accurate.
Thus, if we go towards a certain Reynolds number value for a flow around a cylindrical rod, three-dimensional instabilities appear in the two-dimensional flow. These instabilities are of two types. The so-called 'mode A', Re>188.5 Reynolds numbers, while the 'mode B' appears for larger Re>259 Reynolds numbers. The essential difference between the two modes of instability is the periodicity of the vortex series, the wavelength, i.e. the distance between the vortex series. In the case of mode A instability, the waves repeat at a wavelength $\lambda \approx 4d$, while in mode B instability the waves are denser and the vortices are closer together. In this case, the wavelength, $\lambda \approx 1d$, is approximately one quarter of the wavelength of the mode A instability. There is a transition between the two modes of instability in the range $230<Re<260$, where Re=230 is still dominated by the 'A mode', while Re=260 is dominated by the 'B mode' [2].
Each of the two 3D instability shapes has a characteristic shape, which can be clearly seen in Figure 1.

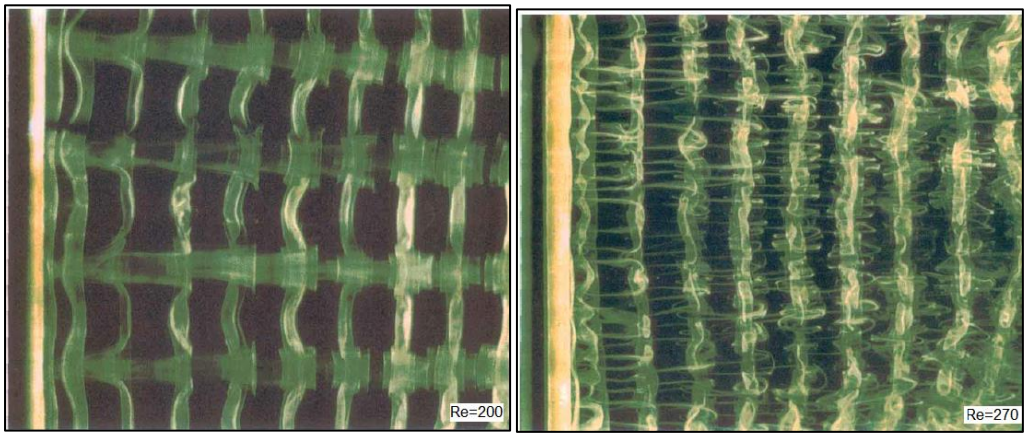

Figure 1. 'Mode A and B' 3D instability, Re=200 and Re=270 [3]

A dye was added to the flowing medium to visualise the instabilities behind the rod. The images show that for mode A instability the vortex lines are approximately $4d$ apart, while for mode B instability $\lambda \approx 1d$.
The images clearly show the spanwise phenomenon under investigation, as 3D instabilities develop along the longitudinal axis of the axis in different cross sections. The aim of our research is to investigate this phenomenon, where we study whether 3D instabilities appear in the two-dimensional flow for a heated rod placed in a wind tunnel under the parameters of our measurement setup. In the following chapters, we present our measurement setup, the equipment used to study the phenomenon, the measurement procedure, and the current directions of development.

2. MEASUREMENT SETUP

In our first measurement, the PIV and the Z-type Schlieren measurement technique were used in parallel. The focus of our investigations was to establish the combined use of both techniques. The test was performed in a closed Göttingen-type wind tunnel. Figure 2 shows a schematic diagram of the implemented measurement setup.

DOI: https://doi.org/10.14232/analecta.2024.3.49-58

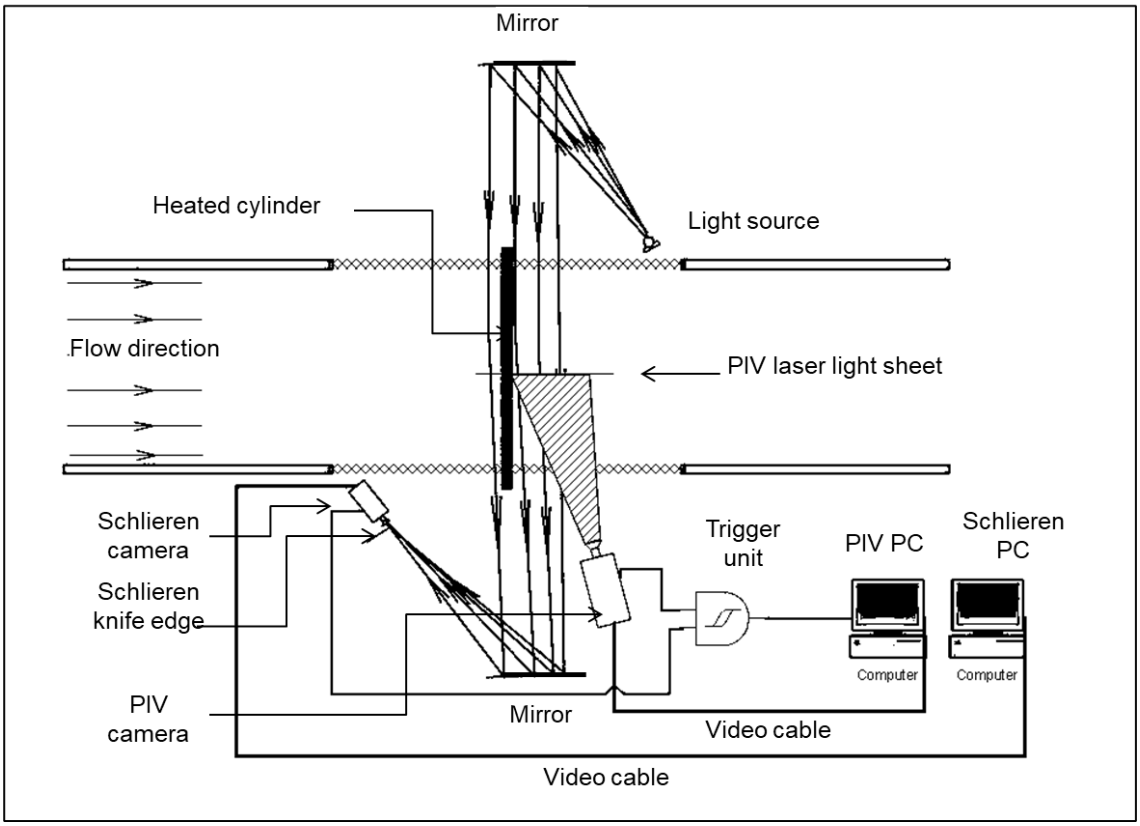

Figure 2. Schematic top view of the measurement system [4]

The measurement setup diagram shows the heated cylinder fixed perpendicular to the flow in a horizontal plane in the 500x500 mm section of the wind tunnel. On both sides of the wind tunnel, in the measuring section, there are transparent glass panels (Figure 3) with holes in the middle to fix the heated rod. The rod has a diameter of d = 10 mm and a length of 500 mm. The rod is electrically heated by means of a toroidal transformer, where the average temperature of the rod during the measurement is set at 300 °C, because the phenomenon under investigation is sufficiently intense at this temperature, which differs considerably from the ambient temperature.

In the PIV measurement, a laser beam illuminates the measurement area $X \times Y$ [mm^2] with light pulses. The particles in the flow are thus illuminated by this laser beam, which is generated by a double pulsed laser. The images are taken with a digital camera that divides the measurement area into pixels according to the sensitivity of the camera, for example $Xp \times Yp$ = 1600×1200 pixels. Depending on the type of camera, a pixel can either detect different shades of grey or different colours. Where the particles are passing by is indicated by a change in hue or colour. The images taken by the camera are enlarged to the original $X \times Y$ [mm^2] size by software installed on the attached computer and divided into small analysis windows, called *IA* iteration areas. The size of an iteration area can be chosen to be $p \times p$ pixels (18×18, 32×32, 64×64, or 128×128).

Iteration areas can be added to cover the area completely, but without overlapping. The quality of image processing can be improved by shooting iteration regions with some overlap. Identical particles in a pair of photographs taken from an iteration window are identified and related by cross correlation. In the cross-correlation process, the intensity (or colour) of each pixel in two images of the iteration space is compared to each pixel in the other image. The result of this statistical comparison (pairing) is the most likely direction

DOI: https://doi.org/10.14232/analecta.2024.3.49-58

and magnitude of the displacement. The correlation mathematical procedure produces a peak signal $R(\Delta x)$, which determines the most likely Δx displacement of identical particles in the two images. This is repeated by the software for each iteration space. To accurately measure the displacement and subsequently determine the velocity, the software applies an interpolation procedure between pixels. This so-called subpixel interpolation means that an interpolation polynomial is applied to the intensity signal sequence detected at the pixels as discrete locations, and the values between pixels are taken into account for cross-correlation. This improves the accuracy of the method. A precise mathematical description of the procedure can be found in the literature [5]. The analysis therefore requires two images from which the displacement can be calculated, but the images also provide a good representation of the flow structure.

"Schlieren" phenomenon refers to the change in direction of light rays passing through optical inhomogeneities. Optical inhomogeneity can occur in gaseous media when the density changes rapidly, so that image distortion occurs due to the deflection of light rays as they pass through. The phenomenon is complex, but in some cases follows well-describable laws, and Schlieren methods can be used to demonstrate and quantify physical phenomena. Schlieren measurement techniques are therefore based on refraction phenomena caused by density changes.

The Z-type Schlieren system uses a point source to ensure good quality images. The different deflections of the light beam from the light source are caused by the index change of refraction due to density changes as the beam passes through a medium of different density. The point light source is focused by lenses/mirrors onto a so-called knife edge or colour filter. Due to the different deflection of the rays passing through different density media, in the case of a knife edge, different brightnesses illuminate the CCD chip of the camera behind the knife edge, while in the case of a colour filter, different colours are input to the chip depending on the amount of deflection. Using a proper calibration procedure, numerical values can be assigned to the temperature field hue [6, 7].

Figure 3. The measurement setup [own photo]

DOI: https://doi.org/10.14232/analecta.2024.3.49-58

The average velocity of the base flow, using a frequency-controlled axial fan, was set to 0.3 m/s, which is the minimum stable base flow that can be produced in a wind tunnel. This low velocity setting was necessary because the measurement method (PIV), which allows the quantitative study of the velocity field, requires a well-defined two-dimensional flow. Therefore, a low Reynolds number flow had to be generated where the flow is approximately two-dimensional. For a rod placed in a wind tunnel, the Reynolds number is Re≈200. The particle image-based measurement technique can be applied reliably in two-dimensional flows, but as previously discussed 3D instabilities can occur in the flow. In our experiment, the Reynolds number stratification is low and the flow can be considered laminar, so we assumed that the flow in the planes perpendicular to the heated rod is nearly identical, i.e. the flow does not vary significantly along the rod axis. This is also a basic requirement for the Schlieren technique.
Although the results of the first measurement were encouraging, they were far from accurate, so the question arose as to how 2D the flow along the longitudinal axis of the rod is, and whether 3D instabilities appear. This is why we started to investigate the spanwise phenomenon, which required a new measurement setup. In the new measurement setup, the laser plane was created at the horizontal centre line of the rod (Figure 4).

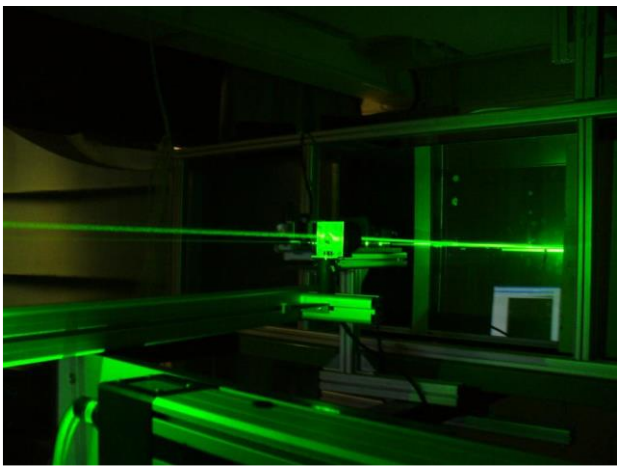

Figure 4. Laser plane optics [own photo]

The results obtained from the evaluation of the measurement are presented in comparison with the numerical simulation results.

3. NUMERICAL SIMULATION

Numerical methods are approximate calculations used to facilitate the solution of differential equations used to describe flow. Of these, the finite volume method is the basis for CFD (Computational of Fluid Dynamics), the numerical simulation of flows. The flow around a heated rod in a wind tunnel was investigated in the Fluent module of the commercially available Ansys software package, which uses the finite volume method. The simulation model has several phases, the first of which is the creation of the geometry model and the numerical mesh. These steps are collectively called the pre-processing of the task, where the real test space is created and mapped to the best possible approximation [8].
In the wind tunnel, the test area is surrounded by a glass wall, where the flow straighteners in the tunnel are trained to create a laminar flow as smooth as possible. The area is 500x500 mm, with the heated rod in the centre of the holes. The test range is divided into different areas for better meshing. The heater rod was modelled based on its catalogue data, the geometric dimensions of which are shown in Figure 5.

DOI: https://doi.org/10.14232/analecta.2024.3.49-58

We first created a two-dimensional version of the model that gave good results, and then used the program to extract the two-dimensional geometry and mesh into a three-dimensional model. In Gambit software, it is therefore possible both to create the necessary geometry and to create the computational mesh.

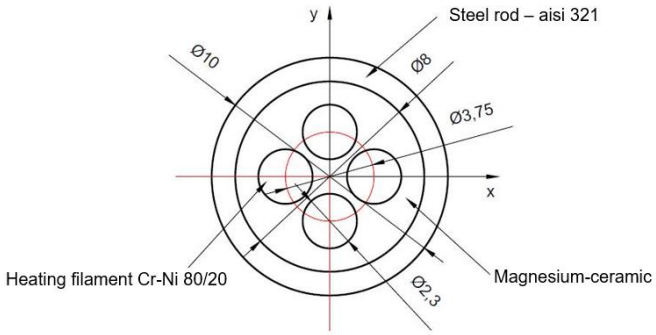

Figure 5. Structure of the heated rod

The centre of the coordinate system is at the centre of the cylinder, from where the upper and lower regions and the input are 7.5*d* away, and the end of the range, the output, is 15*d* away. For the geometric design, a domain of three concentric circles was created, where, where the inner circle is the heated rod, the middle and outer semicircle describe the environment. The design of the central circle and the semi-circular element was chosen for better networkability, while the size of the underlying region was chosen to be 150 mm because this is the only region that can be investigated during measurements. The geometry of the designed calculation domain is shown in Figure 6.

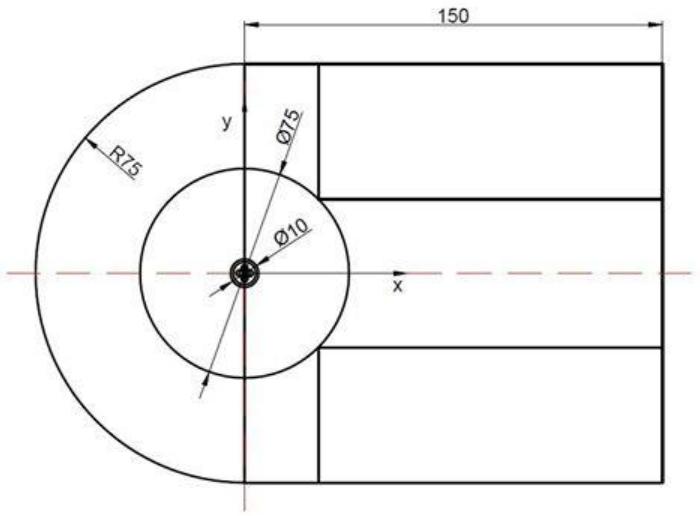

Figure 6. Geometry of the computational space in 2D

The next step is to decompose the drawn geometry into finite volumes from which the numerical mesh is constructed. The surface elements that make up the volumes consist of cell nodes, lines and surface centres. In the construction of the numerical mesh, the aim was to construct the mesh of the space around the circular

DOI: https://doi.org/10.14232/analecta.2024.3.49-58

cylinder being calculated from the simplest possible elements, both to improve computational accuracy and to reduce the computational complexity. In the design of the mesh, we have tried to make the mesh denser where large gradients can be expected, to obtain as detailed a temperature and velocity field as possible, and to avoid sudden changes in size between successive cells, which can cause errors in the calculation. At the same time, it is not advisable to use a dense grid everywhere, as this would only unnecessarily increase the time of the calculation process, while presumably not having a large effect on the final result. Therefore, before building the three-dimensional model, a mesh density test was performed on the two-dimensional model by running simulations to find out the minimum number of elements at which the simulation would still give a realistic result.

The lower and upper surfaces of the rectangular space behind the rod are set to be of the velocity inlet type, avoiding the influence of the vortices behind the rod, since there is no wall in reality. In this case, we also used a denser mesh in the vicinity of the bar, which increases towards the edges of the computational domain. The mesh types are the same as those outlined in the previous model. The computational domain contains 5,740 elements. By extruding the mesh 500 mm in length into three dimensions, the numerical computational mesh shown in Figure 7 is obtained.

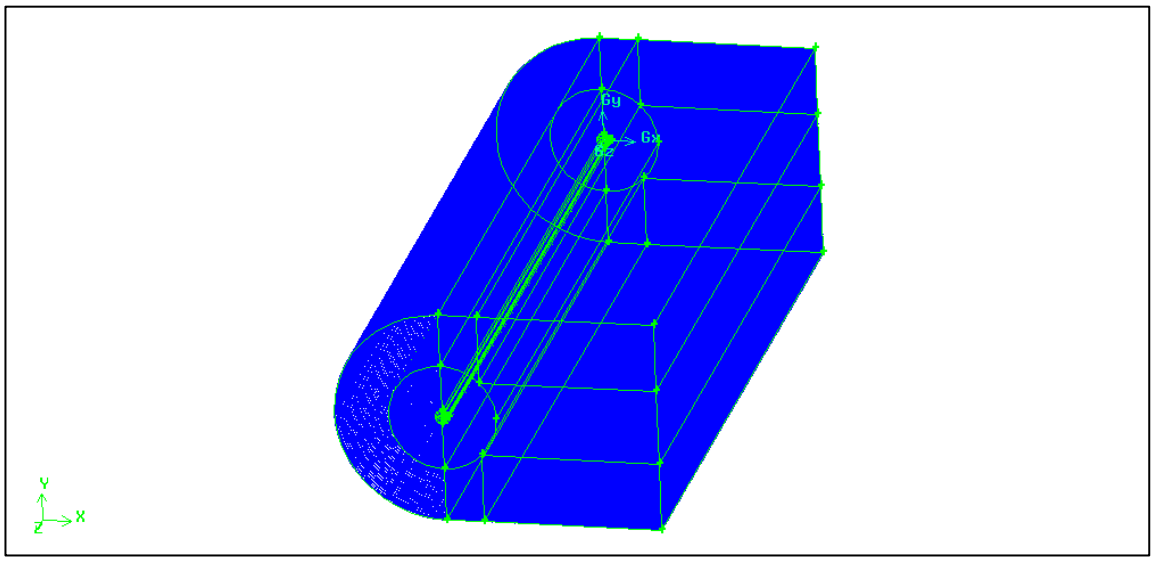

Figure 7. Computational mesh of the 3D model

The number of finite volume elements is 2,870,000 and the mesh quality parameter is 0.478. Unmarked surfaces are automatically treated as 'interfaces' between the same material volume, effectively connecting the two volumes, where the program can easily convert between volumes during the solution. In addition to the boundary surfaces, we have also set the type of each volume, so that the material of the rod and the ceramic and heating filaments within it are solid, while the type of the surrounding volumes is set to fluid, as air flows around the cylinder in the wind tunnel.

During the setup of the simulation in Fluent, the solver models of the equations on which the calculations were based were specified, as well as the material properties of the volumes set in Gambit software and the boundary conditions for the boundary surfaces indicated, and then the initialization process loaded the initial values for each volume. Finally, during iteration, the program solves the corresponding equations. In all cases, the solver models used time-dependent computation for laminar flow using a second-order implicit formulation. For the calculation of the equations of motion and energy I used a second-order procedure. The gravitational force effect was adjusted in all cases.

DOI: https://doi.org/10.14232/analecta.2024.3.49-58

The heating rods were set as a heat source, where the first approach was to set the heat output to 600 W per rod volume in W/m^3, which is of the order of 10^7. However, based on the experience of the test runs, in order to reduce the calculation time and to heat the rod to the desired temperature more quickly, the magnitude was increased by one to 10^8. This did not affect the accuracy of the results, as the aim was to achieve an average rod surface temperature of 300 °C, and by reaching this temperature sooner during the run, the phenomena in the underlying range were not affected.
In all cases, the change in air viscosity is calculated according to 'Sutherland's law'. In the 3D model, the 'pressure based' mode, an incompressible ideal gas setting, was used. For the boundary conditions, a velocity of 0.3 m/s was entered for the 'velocity inlet' surface, which is the wind speed set in the wind tunnel during the measurements. The 'simple' method was used to calculate the velocity-pressure relationship and the 'second order' method was used to interpolate the pressure.

3. RESULTS AND DISCUSSION

The results obtained in the three-dimensional model were evaluated in the CFD-Post module of the Ansys software package. In a first step, a plane was created at the centre of the rod (z=0.25 m), on which the temperature and the vorticity distribution were plotted. Figure 8 illustrates the position of the created plane, where the temperature distribution of that plane is displayed.

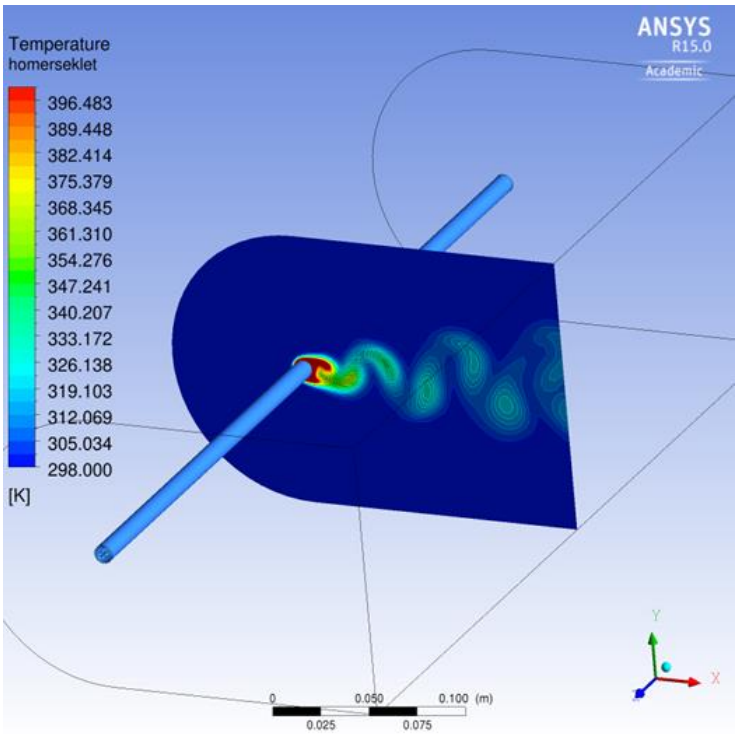

Figure 8. The temperature distribution in the z=0,25 m plane

In Figure 8, where the local temperature values are plotted along the length of the rod perpendicular to the longitudinal axis at z=0.25 m, y=0, x is plotted along the entire computational domain, and plotted on a line graph. Also plotted along the same line are the vortex spacing frequency values at each point, showing that the vortex cores coincide with the highest temperature points in the heat packs.

DOI: https://doi.org/10.14232/analecta.2024.3.49-58

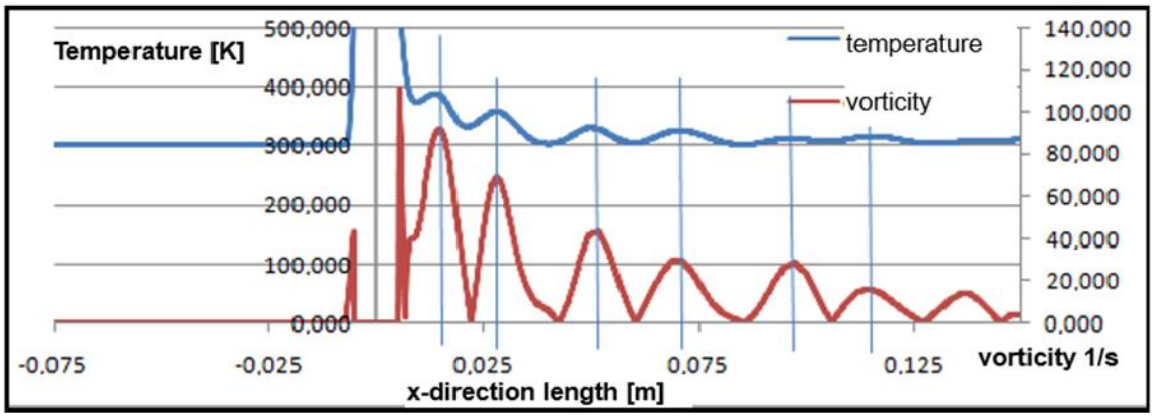

Figure 8. Coincidence of heat packets and vortex cores

The PIV measurements carried out to investigate the spanwise phenomenon are performed in several planes, of which the velocity field along the centre line of the rod at y=0 in the xz plane, displayed from the evaluated data for the rod heated to 300 °C, is shown in Figure 9. The rod is not marked in the figure, only the underlying space is shown. The figure does not show the full cross-section because the optics positioned towards the wind tunnel were only able to capture this much of the image at that distance. Figure 9 shows the velocity distribution obtained from the numerical simulation over the full cross section of the measurement domain.

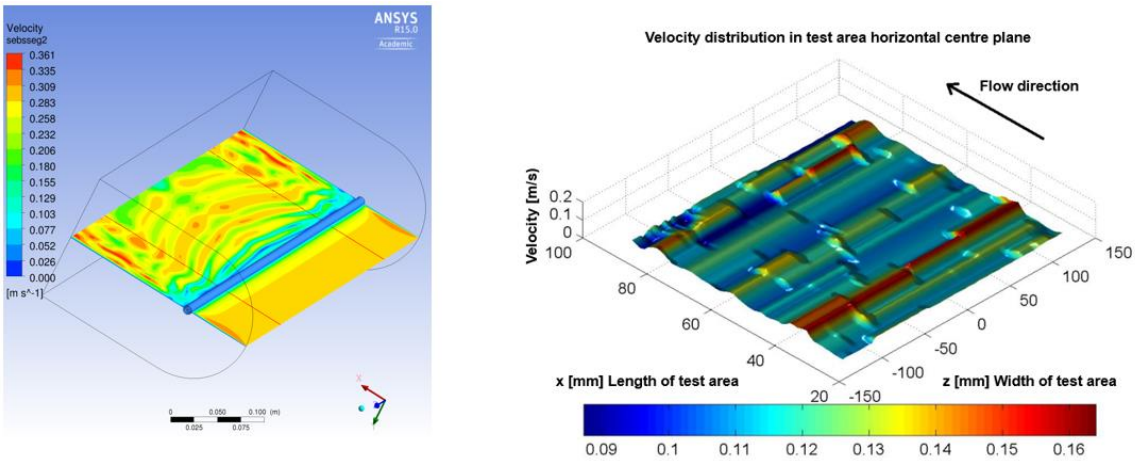

Figure 9. Raw velocity image from numerical simulation and PIV measurement at a rod temperature of 300 °C

4. CONCLUSIONS

Figure 8 shows that the numerical simulation also indicates that there is a clear relationship between the eddy distribution measured in a cross section and the average temperature distribution obtained as a cross section, but that the two distributions are not expected to be fully synchronous. The difference between the two distributions during measurements is also magnified by other uncertainties due to the measurement procedures (different sensitivity of the measuring instruments, calibration errors of the measurement results, distorting effects of camera optics, non 100% homogeneity of the tunnel flow, etc.). However, numerical

DOI: https://doi.org/10.14232/analecta.2024.3.49-58

simulations and measurements have in all cases confirmed, with varying degrees of accuracy, our basic assumption that the heat leaving the heated rod surface as a result of the combined effect of free and forced convection leaves the cylinder in the form of so-called "heat packets" with the same frequency as the vortex separation frequency.
Based on Figure 9, the following conclusions can be made: the regular vortex separation breaks up near the walls. A quasi 2D flow develops away from the walls, the vortices are periodically separated, but the vortex centres are not straight lines parallel to the rod, but curved. Based on the results, it can be seen that the effect of the spanwise phenomenon has been demonstrated, both from the measurement and numerical simulation results.

REFERENCES

[1] Bolló B., Fűtött körhenger körüli áramlás vizsgálata, GÉP 63:(1) (2012), pp. 31-34.
[2] B. Dwight, R. D. Henderson, Three-dimensional Floquet stability analysis of the wake of a circular cylinder, Journal of Fluid Mechanics 322 (1996), pp. 215-241.
[3] Williamson, C. H. K., Three-dimensional wake transition, Journal of fluid mechanics 328 (1996), pp. 345-407.
[4] P. Bencs, Sz. Szabó, D. Oertel, Simultaneous measurement of velocity and temperature field in the downstream region of a heated cylinder, Engineering Review 34.1 (2014), pp. 7-13.
[5] B. Paripás, Sz. Szabó, Lézeres mérési és megmunkálási eljárások a gépészetben, Nemzeti Tankönyvkiadó (2009) pp. 66-67.
[6] Bencs P., Szabó Sz., Instacionárius léghőmérsékletmező mérési lehetőségeinek fejlesztése, GÉP LXIII.: (1.) (2012), pp. 27-30.
[7] P. Bencs, Sz. Szabó, R. Bordás, K. Zähringer, D. Thévenin, Simultaneous measurement of velocity and temperature downstream of a heated cylinder. Pressure Vessels and Piping Conference. Vol. 44571. (2011), pp. 207-212.
[8] Fluent, A. N. S. Y. S., Ansys fluent theory guide, Ansys Inc., USA 15317 (2011), pp. 724-746.

DOI: https://doi.org/10.14232/analecta.2024.3.49-58